

Cortical Morphometry in the Psychosis Risk Period: A Comprehensive Perspective of Surface Features

Supplemental Information

A Comprehensive Review of Existing Literature

While a body of CSM literature indicates aberrant brain characteristics in schizophrenia, including local gyrification index (*IGI*), curvature, and sulcal depth (1-3); there are varying reports of widespread differences related to schizophrenia with little anatomical specificity (4-5). These schizophrenia (SZ) findings include asymmetric sulcal depth in temporal lobes (6; SZ, n=33), widespread frontal hyper-gyrification as measured by *IGI* (7; SZ n=57), and hypogyrfication in frontal lobes, posterior lobes based on gyrification index (8; SZ n=9). Inconsistencies in the direction and localization of these effects leave ambiguity as to whether these markers reflect a single hit in utero, degenerative process/environmental stressors, or by methodological effects (i.e, small effect sizes combined with individual variability; 9).

In contrast to the large body of evidence in schizophrenia populations, studies in populations with either clinical or genetic risk for psychosis are limited. Of the literature that does exist, this work suggests that CSM abnormalities are prevalent in these groups (9-13). Specifically, abnormal cortical folding (i.e., gyrification index) in the right prefrontal cortex relates to genetic high risk for psychosis (n=128), which was particularly abnormal in converters prior onset of psychosis (n=17), and in first episode patients (FEP) (n=34) (9-10,14). Similar analysis of CHR (n=104) and those who later converted to psychosis (n=21), had significantly different cortical folding (*IGI*; 13). Sasabayashi et al. (2017b) extended this research to FEP (n=62), finding widespread *IGI* differences, including frontal, temporal, and parietal lobes (15). Taken together data from Harris et al., (2004, 2007) and Sasabayashi et al., (2017a, b) suggest that gyrification may be a particularly useful marker of early risk as well as a predictor of progression to psychosis (9-10,13,15).

Another set of important studies compared groups of healthy controls, CHR (n=18) to 22q11-deletion syndrome (n=18) – a genetic disorder with 30% lifetime risk of psychosis - and there were no observed differences in *IGI* between CHR and healthy controls, but significant differences in the 22q11-deletion syndrome (16). Difference in *IGI* also relate to negative symptoms in patients in 22q11.2-deletion syndrome (n=71; 17). Similarly, in a study of CHR participants (n=24), researchers found that aberrant patterns of gyrification (both hypo- and hyper-gyrification; *IGI*) were among the markers that predicted symptom severity at clinical follow-up (18). Finally, only one study examined the olfactory sulci in FEP (n=64) also found abnormal sulcal depth compared to controls that related to deficits in executive function (19). While collectively these investigations point out CSM abnormalities in this critical period, to date no studies have employed multiple imaging time points or included multiple CSM features to provide a comprehensive perspective of these cortical features (See below for a comparison of the relative advantages of each metric).

A Comprehensive Perspective of Cortical Surface Morphometry

The current study evaluates the local gyrification index (*IGI*). A majority of other extant studies employed the simpler gyrification index (*GI*), which while informative, relies on a two-dimensional ratio of the length of the inner contour of the cortical surface to the length of the outer contour (20). In contrast, local gyrification index (*IGI*) is a ratio of all hidden cortex to all outer cortex, i.e. a smooth surface hemifield. *IGI* employs advanced computation that allows the metric to consider more cortical features taking into account three-dimensions of gyrification rather than relying on a single orientation (20-21). Further, *IGI* provides additional sensitivity to variation due to slice orientation and the presence of buried sulci, which increasing the precision in localizing gyral abnormalities (21).

While the *IGI* provides invaluable information, it references an individualized contour; taking this approach in isolation may obscure the exact nature of the specific gyral morphometry. A solution to this issue may lie in incorporating additional measures such as mean curvature index (*MCI*). *MCI* quantifies each point on the surface in terms of the radius of osculating circles from the peak of each gyrus. This

means that if the radius gets smaller as it approaches the gyrus, then the gyrus has a sharper point and a higher MCI value (22). This CSM metric provides further sensitivity to changes on a smaller scale, and information about the shape of a given arch, (i.e. higher MCI implies a sharper curve while lower numbers represent a wider arch; 23). Unfortunately, this promising index has not been used in CHR youth.

Finally, sulcal depth provides unique and complimentary estimates of linear distance from a middle gyrification point, (i.e. the global midpoint between the gyri and sulci; 24). Similar to */GI*, sulcal depth is based on a custom reference to each individual's hemi-curvature. However, in */GI* the individualized reference is the outer cortical surface contour, but in sulcal depth it references the midpoint surface (i.e., the linear distance provides from this individualized metric). Thus, incorporating three metrics provides a more comprehensive and nuanced perspective which includes an inner/outer surface ratio, a curve reference, and linear height/depth.

Participants

A total of 81 participants (CHR=43, HC=38) were recruited through the Adolescent Development and Preventive Treatment (ADAPT) Program. All participants were recruited using newspaper and media announcements, bus advertisements, Craigslist, and flyers. CHR inclusion criteria was based on the presence of a prodromal syndrome (25), and not genetic risk. Exclusion criteria for all participants included: a history of a significant head injury or other physical disorder affecting brain functioning, contraindications to the magnetic imaging environment, mental retardation defined by an IQ of less than 70, and substance dependence in the past 6 months. CHR exclusion criteria included any Axis I psychotic disorder diagnosis (e.g. schizophrenia, schizoaffective, bipolar disorder with psychotic features). Control exclusion criteria included any Axis I diagnosis or a first-degree relative with psychosis to generate similarly low genetic risk among all subjects. Demographic and positive symptoms characteristics of the sample are described in Table 1.

Clinical Interviews

The Structured Interview for Prodromal Syndromes (SIPS; 25) diagnosed CHR syndromes. The Structured Clinical Interview for the DSM-IV (SCID, research version), ruled out Axis I psychotic disorders and substance dependence. Interviewers (advanced doctoral students) trained for 2-months, and inter-rater reliabilities exceeded the minimum study criterion of $Kappa \geq .80$. Participants were also given the Word Reading subtest of the fourth edition of the Wide Range Achievement Test (WRAT) as a measure of general intelligence. The WRAT is well-validated and broadly used measure of achievement and broad learning ability for adolescents and young adults (28).

Scanning Procedures

All participants completed a structural scan, resting state functional connectivity MRI, and DTI scans. A 3-Tesla Siemens Tim Trio MRI Scanner (Siemens AG, Munich, Germany) using a standard 12-channel head coil acquired the scans. Structural images were a T1-weighted 3D magnetization prepared rapid gradient multi-echo sequence (MPRAGE; sagittal plane; repetition time [TR] 2,530 ms; echo times [TE] 51.64 ms, 3.5 ms, 5.36 ms, 7.22 ms, 9.08 ms; GRAPPA parallel imaging factor of 2; 1 mm³ isotropic voxels, 192 interleaved slices; FOV 525 6 mm; flip angle 57).

Data Preprocessing and Analysis

FreeSurfer version 5.3.0 automatic segmentation software extracted cortical surface definitions (<http://surfer.nmr.mgh.harvard.edu/>; 24). Specifically, morphometric measurements were obtained by reconstructing representations of the gray/white matter boundaries. For group analyses, a study specific space was generated from these individual surfaces consistent with past studies (24). Individual surfaces were averaged using a non-rigid, high-dimensional spherical method that relies on the alignment of cortical folding patterns. Using cortical folding patterns generates a study specific space that maximizes the accuracy of the morphological alignment of homologous cortical locations based on individually defined anatomical landmarks, while minimizing metric distortion. Each participant was registered to a

study-specific template and smoothed using a Gaussian kernel of 10 mm prior to group analysis, and corrected with False Discovery Rate (FDR) of $p < .05$ to correct for multiple comparisons, consistent with the analyses recommendations of Schaer et al. (2012) (21). Query Design Estimate Contrast tool (QDEC) in the FreeSurfer program generated the group contrasts in a general linear model controlling for gender and medication status, and compared MCI, and sulcal depth at each vertex. Local gyrification index was calculated using the general linear model tools (21). Query Design Estimate Contrast tool (QDEC) in the FreeSurfer program generated the group contrasts in a repeated measure ANOVA controlling for gender and medication status, and compared MCI, and sulcal depth at each vertex. Local gyrification index was calculated using the general linear model tools (21).

Demographic Characteristics and Clinical Symptoms

Group differences in demographic characteristics were examined with independent t-tests and chi-square tests. There were no significant between-group differences in demographic characteristics such as age, $t(74) = -.49$, $p = .63$, participant education, $t(70) = -1.04$, $p = .30$, and parental education $t(79) = -.80$, $p = .94$. There was, however, a difference in the distribution of gender in our sample, $\chi^2(1) = 7.71$, $p = .005$. Accordingly, the following analyses control for gender. As expected, the CHR group showed significantly more positive symptoms, the defining feature of the prodrome (23), at baseline $t(1,79) = 18.23$, $p \leq .001$ and at the 12 month follow-up $t(1,79) = 10.44$, $p \leq .001$. A total of 8 CHR participants (18.6%) were treated with antipsychotic medication; this was also treated as a nuisance covariate. Of the total of 8 participants that were on antipsychotic medications, the average chlorpromazine equivalent was 112.50 (SD=53.68) for time 1 and 75 (31.92) for time 2. There were no significant differences in CPZ equivalent between time points, $t(8) = .382$, $p = .25$. Data summarized in *Table 1*.

Exploratory examination of symptoms relationships. CSM features from the peak cluster were extracted from each hemisphere and related to the positive and negative symptoms at the corresponding time point. The only relationship of note, was a trending relationship between negative symptoms and mean curvature index in the left ($r(42) = 0.30$, $p = 0.02$) and right ($r(42) = 0.21$, $p = 0.04$) hemisphere, which

did not survive correction for multiple comparison for these twelve exploratory analyses. See *Supplemental Table S3*.

Comparison of Cortical Surface Morphometry (CSM) Metric Convergence and Uniqueness

To evaluate whether CSM clusters converge on vertices or identify unique vertices of surface morphometry, significant clusters were overlaid and compared pairwise; generating two unique masks: a convergence map- containing vertices where metrics converge on CSM abnormalities, and a uniqueness map- demonstrating the unique information provided by each metric (Table 5, Figure 4). Convergence only occurred between two metrics, MCI (19.5% of vertices overlap in the left hemisphere; 28.72% of vertices overlap in the right hemisphere) and abnormal sulcal depth (34.61% of vertices overlap in the left hemisphere; 26.44% of vertices overlap in the right hemisphere). Converging regions across these metrics were particularly significant, and so it is unsurprising that multiple metrics of CSM metrics were sensitive to these highly aberrant features. There were, however, significant points of divergence in the data suggesting that each distinct metric identifies unique sites of abnormal development. In fact, 100% of *IGI* clusters were unique to this metric. Further, while there was notable overlap between the MCI and sulcal depth metrics, each metric provided a large amount of unique information; MCI represented 76.4% unique cluster information and sulcal depth contained 70.35% unique clusters. Qualitatively, while the ratio metric of *IGI* demonstrates distinct gyrification in frontal and temporal regions, the geometric distance and shape metrics, MCI and sulcal depth, clusters were primarily in parietal, occipital, and cingulate regions, see *Supplemental Table S1*.

Stability of CSM Metrics Over Time

To use both time points as a converging data point, we must test the assumption that the gyrification is stable over time. This also provides us with a unique opportunity to confirm the stability of gyrification, and assessing whether these metrics change during the prodromal period. To examine gyrification stability, an Inter-Class Correlation (ICC) compared the CSM metrics for each time point for

significant clusters to reduce the number of comparisons to the relevant vertices discussed below. These analyses treat FreeSurfer's standardized algorithm as a single, stable rater of CSM metrics in a fixed-rater model of class correlation, which was used in the Psych Package of R v.3.1.2 (29). While Cronbach's Alpha is typically reported Guttman's Lambda has been reported here as it better takes into account the variance of the data (29). See *Supplemental Figure S1* for a depiction of peak clusters by group over time. Across all subjects the CSM metrics were significantly and highly stable over time. Each IGI significant cluster's ICC ranged from .73-.83, all p 's<.05. Similar stability was demonstrated across clusters in MCI, with each significant cluster's ICC ranging from .67-.88, all p 's<.05. Finally, sulcal depth stability across each significant cluster ranged in ICC from .70-.97, all p 's<.05. To measure the consistency of the CSM metrics across each significant cluster an overall metric of prenatal development, measured the consistency of whole brain clusters into a Guttman's Lambda (Λ) for each metric (For more information on this metric see above). These measures were also highly reliable, IGI (Λ =.92), MCI (Λ =.86), and sulcal depth (Λ =.93). In parallel analyses, the CHR group did not significantly differ in the stability of their CSM, see *Supplemental Table S2*. The stability of CSM features over time is consistent with the notion that these features develop in utero and is largely immune to changes related to later environmental and developmental factors.

Supplemental Table S1. Percentage Spatial Cluster Overlap of CSM Metrics by Group

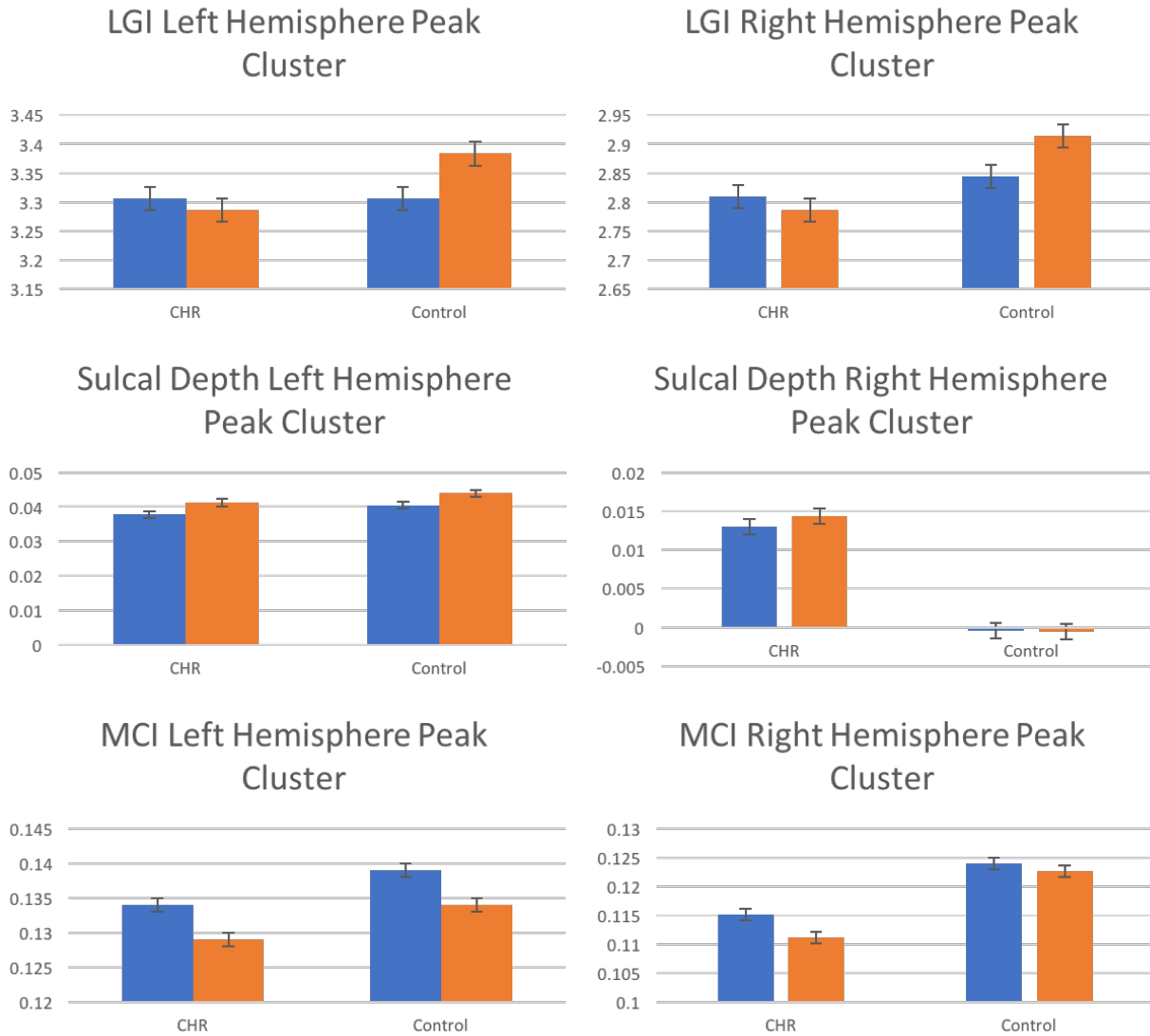
Metric	Cluster Overlap	
	Left	Right
MCI	34.6%	26.44%
Sulcal Depth	19.5%	28.72%
<i>IGI</i>	0%	0%

Supplemental Table S2. ICC of CSM Metrics by Group

Metric	ICC Group	
	CHR	HC
<i>IGI</i>	.64-.80	.68-.80
MCI	.64-.84	.64-.86
Sulcal Depth	.67-.95	.67-.95

Supplemental Table S3. Relationship of Peak Clusters to Symptoms

Symptom	Sulcal Depth		Mean Curvature Index		Local Gyrification Index	
	Left	Right	Left	Right	Left	Right
Positive Symptoms (Baseline)	-0.07	-0.1	0.05	0.15	0.18	-0.13
Positive Symptoms (Follow Up)	-0.02	-0.07	0.05	0.14	0.14	0.01
Positive Symptoms (Repeated Measure Correlation)	r(42)=-.09	r(42)= .10	r(42)=.19	r(42)= .15	r(42)= .023	r(42)= .16
Negative Symptoms (Baseline)	-0.26	-0.52	-0.13	0.17	0.07	-0.2
Negative Symptoms (Follow Up)	-0.06	-0.36	-0.01	0.16	0.16	0.14
Negative Symptoms (Repeated Measure Correlation)	r(42)=0.004	r(42)=-0.16	r(42)=0.305 ⁺	r(42)=0.34 ⁺	r(42)=0.212	r(42)=0.02



Supplemental Figure S1. Uncorrected Peak Clusters by Group and Time-Point: To demonstrate stability of raw, uncorrected metrics, the group differences are plotted for each peak cluster by group for Baseline (blue) and Follow-Up (Orange).

Supplemental References

1. Csernansky, J. G., Gillespie, S. K., Dierker, D. L., Anticevic, A., Wang, L., et al. (2008). Symmetric abnormalities in sulcal patterning in schizophrenia. *NeuroImage*, *43*(3), 440–446. <https://doi.org/10.1016/j.neuroimage.2008.07.034>
2. Kulynych, J. J., Luevano, L. F., Jones, D. W., & Weinberger, D. R. (1997). Cortical abnormality in schizophrenia: An in vitro application of the gyrification index. *Biological Psychiatry*, *41*(10), 995–999. [https://doi.org/10.1016/S0006-3223\(96\)00292-2](https://doi.org/10.1016/S0006-3223(96)00292-2)
3. Palaniyappan, L., Mallikarjun, P., Joseph, V., White, T. P., & Liddle, P. F. (2011). Folding of the prefrontal cortex in schizophrenia: Regional differences in gyrification. *Biological Psychiatry*, *69*(10), 974–979. <https://doi.org/10.1016/j.biopsych.2010.12.012>
4. deWit, S., Ziermans, T. B., Nieuwenhuis, M., Schothorst, P. F., van Engeland, H., Kahn, R. S., et al. (2017). Individual prediction of long-term outcome in adolescents at ultra-high risk for psychosis: Applying machine learning techniques to brain imaging data. *Human Brain Mapping*, *38*(2), 704–714. <https://doi.org/10.1002/hbm.23410>
5. Mihailov, A., Padula, M. C., Scariati, E., Schaer, M., & Eliez, S. (2017). Morphological brain changes associated with negative symptoms in patients with 22q11.2 Deletion Syndrome. *Schizophrenia Research*, *188*, 52–58.
6. Narr, K. L., Toga, A. W., Szeszko, P., Thompson, P. M., Woods, R. P., Robinson, D., et al. (2005). Cortical thinning in cingulate and occipital cortices in first episode schizophrenia. *Biological Psychiatry*, *58*(1), 32–40. <https://doi.org/10.1016/j.biopsych.2005.03.043>
7. Harris, J. M., Whalley, H., Yates, S., Miller, P., Johnstone, E. C., & Lawrie, S. M. (2004). Abnormal cortical folding in high-risk individuals: A predictor of the development of schizophrenia? *Biological Psychiatry*, *56*(3), 182–189. <https://doi.org/10.1016/j.biopsych.2004.04.007>
8. Harris, J. M., Yates, S., Miller, P., Best, J. J. K., Johnstone, E. C., & Lawrie, S. M. (2004). Gyrification in first-episode schizophrenia: A morphometric study. *Biological Psychiatry*, *55*(2), 141–147. [https://doi.org/10.1016/S0006-3223\(03\)00789-3](https://doi.org/10.1016/S0006-3223(03)00789-3)
9. Jung, W. H., Kim, J. S., Jang, J. H., Choi, J. S., Jung, M. H., Park, J. Y., & Kwon, J. S. (2011). Cortical thickness reduction in individuals at ultra-high-risk for psychosis. *Schizophrenia Bulletin*, *37*(4), 839–849. <https://doi.org/10.1093/schbul/sbp151>
10. Cannon, T. D., Chung, Y., He, G., Sun, D., Jacobson, A., Van Erp, T. G. M., et al. (2015). Progressive reduction in cortical thickness as psychosis develops: A multisite longitudinal neuroimaging study of youth at elevated clinical risk. *Biological Psychiatry*.
11. Harris, J. M., Moorhead, T. W. J., Miller, P., McIntosh, A. M., Bonnici, H. M., Owens, D. G. C., Lawrie, S. M. (2007). Increased prefrontal gyrification in a large high-risk cohort characterizes those who develop schizophrenia and reflects abnormal prefrontal development. *Biological Psychiatry*, *62*(7), 722–729. <https://doi.org/10.1016/j.biopsych.2006.11.027>
12. Sasabayasi, D., Takayanagi, T., Koike, S., Yamasue, H., Naoyuki, K., Sakuma, A., et al. (2017). Increased occipital gyrification and development of psychosis disorders in individuals with an at-risk mental state: A multicenter study. *Biological Psychiatry* (82)10, 737–745.
13. Sasabayasi, D., Takayangagi, Y., Nishiyama, S., Takahasi, T., Furuichi, A., Kido, M., et al. (2017). Increased frontal gyrification negatively correlates with executive function in patients with first-episode schizophrenia. *Cerebral Cortex*, *27*(4), 2686–2694. <https://doi.org/10.1093/cercor/bhw101>.

14. Bakker, G., Caan, M. W. A., Vingerhoets, W. A. M., Da Silva-Alves, F., De Koning, M., Boot, E., et al. (2016). Cortical morphology differences in subjects at increased vulnerability for developing a psychotic disorder: A comparison between subjects with ultra-high risk and 22q11.2 deletion syndrome. *PLoS ONE*, *11*(11), 1–16. <https://doi.org/10.1371/journal.pone.0159928>
15. Insel, T. R. (2010). Rethinking schizophrenia. *Nature*, *468*(7321), 187–193. <https://doi.org/10.1038/nature09552>
16. Jørgensen, K. N., Nesvåg, R., Gunleiksrud, S., Raballo, A., Jönsson, E. G., & Agartz, I. First- and second-generation antipsychotic drug treatment and subcortical brain morphology in schizophrenia. *Eur Arch Psychiatry Clin Neurosci* *266*(5): 451-460.
17. Takahashi, T., Nakamura, Y., Nakamura, K., Ikeda, E., Furuichi, A., Kido, M., et al. (2013). Altered depth of the olfactory sulcus in first-episode schizophrenia. *Prog Neuropsychopharmacol Biol Psychiatry*, *40*, 167-172.
18. Zilles, K., Armstrong, E., Schleicher, A., & Kretschmann, H. (1988). The human pattern of gyrification in the cerebral cortex. *Anatomy and Embryology*, *179*(2), 173-179.
19. Schaer, M., Cuadra, M. B., Schmansky, N., Fischl, B., Thiran, J.P., & Eliez, S. (2012). How to measure cortical folding from MR images: A step-by-step tutorial to compute local gyrification index. *Journal of Visualized Experiments*, (59), 1–10. <https://doi.org/10.3791/3417>
20. Pienaar, R., Fischl, B., Caviness, V., Makris, N., & Grant, P. E. (2008). A methodology for analyzing curvature in the developing brain from preterm to adult. *International journal of Imaging Systems and Technology*, *18*(1), 42-68.
21. Luders, E., Thompson, P. M., Narr, K. L., Toga, A. W., Jancke, L., & Gaser, C. (2006). A curvature-based approach to estimate local gyrification on the cortical surface. *Neuroimage*, *29*, 4, 1224-1230.
22. Fischl, B. (2012). Freesurfer. *Neuroimage*, *62*(2), 774-781.
23. Miller, T. J., McGlashan, T. H., Rosen, J. L., Cadenhead, K., Ventura, J., McFarlane, W., & Woods, S. W. (2003). Prodromal assessment with the structured interview for prodromal syndromes and the scale of prodromal symptoms: Predictive validity, interrater reliability, and training to reliability. *Schizophrenia Bulletin*, *29*(4). <https://doi.org/10.1093/oxfordjournals.schbul.a007040>
24. Miller, T. J., McGlashan, T. H., Woods, S. W., Stein, K., Driesen, N., Corcoran, C. M., et al. (1999). Symptom assessment in schizophrenic prodromal states. *Psychiatric Quarterly*, *70*(4), 273–287.
25. Friston, K. J., & Frith, C. D. (1995). Schizophrenia: A disconnection syndrome? *Clinical Neuroscience (New York, N.Y.)*, *3*(2), 89–97.
26. Wilkinson, G. S., & Robertson, G. J. (2006). Wide range achievement test 4 (WRAT4). *Psychological Assessment Resources*.
27. Revelle, W., (2017). Package “psych.” Retrieved, 2017, from http://personality-project.org/r/psych_manual.pdf